

Theo DuBose Thesis

Theo DuBose

April 18, 2012

Part I

Immunospecific Gold Nanoparticles for Contrast Enhancement of Corneal Tissue Culture

1 Introduction

According to the National Eye Institute (NEI), approximately 40,000 cornea transplants are performed every year in the United States. Unfortunately, about 20 percent (8000 per year) of these transplants are rejected [5], necessitating a second transplant. An increase in the number of procedures is inconvenient for the patient at best; therefore, it is desirable to find ways to minimize the amount of rejection as well as increase the overall supply of tissue for cornea transplants.

1.1 Corneal Engineering

Prof. Liz Orwin's lab at Harvey Mudd College is attempting to overcome the challenges of cornea transplants by growing replacement corneas. This is done by electrospinning collagen fibers, then seeding cells from a patient who needs new corneas. However, the electrospun collagen does not possess the structural properties of corneal collagen, so the Orwin Lab is focused on finding ways to control the phenotype and regulatory mechanisms of the cells. It is hoped that through this process, the cells will reenact the initial formation of the corneas in fetal development, taking up the electrospun collagen and laying it back down in the native form, viz., a hexagonal close-packed array of 30 nm-diameter collagen fibrils.

In order to better understand the behavior of the cells in response to the treatments they receive, Prof. Orwin's lab would like to be able to monitor both the position and phenotype of the cells in the scaffold. Confocal microscopy, a standard biological imaging modality, has a high ($< 1 \mu\text{m}$ isotropic) resolution but can only image $25 \mu\text{m}$ deep. The high resolution makes confocal desirable, but human corneas are $500 \mu\text{m}$ thick, and the collagen scaffolds can be thicker, making confocal unusable for full 3D imaging. In contrast, the optical coherence microscope (OCM) trades high resolution ($5 \mu\text{m}$ lateral, $10 \mu\text{m}$ axial) for over 1 mm of depth penetration at 850 nm. Consequently, the OCM was employed to monitor the cells.

Unfortunately, the collagen in the scaffold scatters too highly for the OCM to distinguish the cells, so Chris Raub '04 proposed a method, developed from a paper by Sokolov [11], wherein 35 nm gold nanoparticles would be applied to increase scattering of the cells via a process called indirect immunolabeling, the basic precepts of which are still used in this project [10]. Indirect immunolabeling has four key components: a target protein (we are targeting $\alpha 5 \beta 1$ -integrin), a primary antibody that is *anti*- the target protein (MAB1999), a secondary antibody that is *anti*- the primary antibody (AP124F), and a label (both the gold nanoparticles and a fluorescent molecule on the AP124F). Indirect immunolabeling is implemented by first binding primary antibodies (Ab1) specific to surface proteins on corneal cells to those surface proteins. Then, secondary antibodies (anti-Ab1) are bound to nanoparticles via Van der Waals forces. The antibody-gold is then allowed to then bind to the Ab1-protein-cell *in vitro*. A schematic diagram of this process is shown in Figure 1.

Jamie Shoffeit '05 [1], Megan Arman '06, and Emily Hogan '07 all followed on Raub's work to achieve labeling. The process they consisted of creating 35 nm diameter gold nanoparticles from a citrate reduction of Au(III) and binding the antibodies to the nanoparticles via Van der Waals forces alone. Although Hogan was finally able to use this technique to produce a statistically significant increase in scattering in 2007, the scattering increase was not as great as was desired.

To address this, David Coats '08 did a number of studies to optimize the gold being used as the labeling agent. Coats performed extensive calculations using Mie theory to

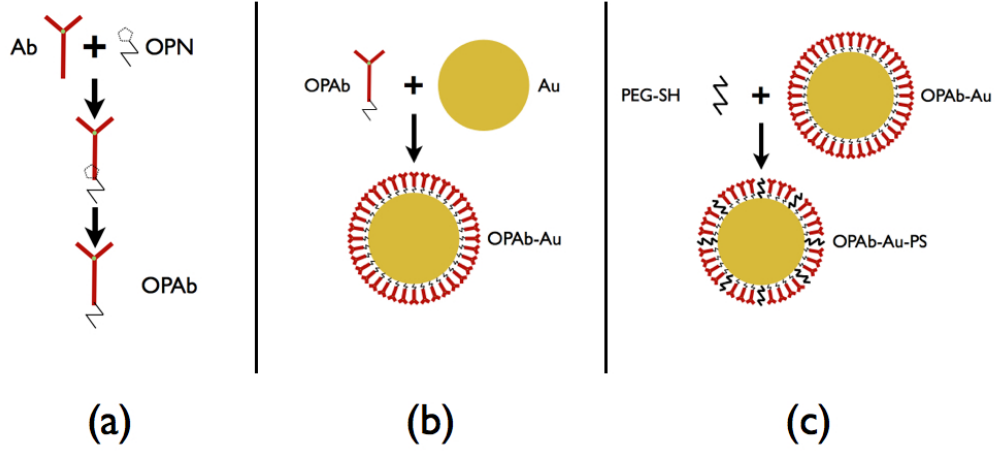


Figure 1: Stages of indirect immunolabeling presented schematically (not to scale). (a) The primary antibody, MAB199, binds to the targeted surface protein, $\alpha 5\beta 1$ -integrin. (b) Secondary antibodies, AP124F, are bound to the surface of a gold nanoparticle. (c) A gold nanoparticle-secondary antibody complex binds to the primary antibody, which in turn is bound to the surface protein.

maximize scattering. Mie theory details the scattering pattern of particles on the order of or larger than the wavelength of light they scatter. As even a 35 nm nanoparticle cannot be approximated as a point when using 850 nm light, Mie theory provides a far more accurate prediction of the intensity of backscattered intensity than Rayleigh scattering theory. These calculations showed that for any diameter, a particle made of solid gold (versus a particle with an inner core of silica) gave the highest scattering to absorption cross-section ratio, as shown in Figure 2. As can also be seen in that image, C_{sca}/C_{abs} also increases with diameter, up to a point. However, the settling rate of the gold particles also had to be taken into account, as well as the availability of manufactured gold nanoparticles. With these multiple factors in consideration, it was decided that 90 nm diameter nanoparticles from Nanopartz would be used. With these improved gold particles, David Coats again performed imaging tests on a monolayer of cells. However, the same lack of obvious signal generation prompted even further investigation.

One concern regarding the labeling system was that the antibodies were bound to the gold with only van der Waals forces. Rob Warren '10 [13] discovered a procedure in a paper by Lowery et al. [7] by which increased binding had been achieved for immunolabeling. The

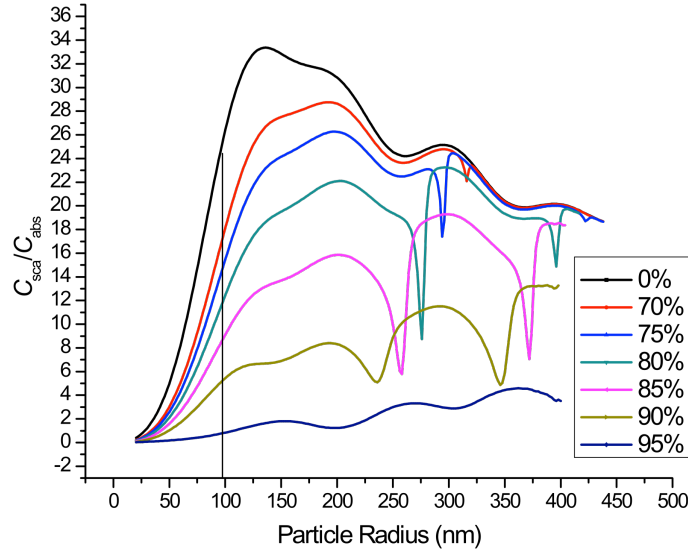


Figure 2: Plot of ratio of scattering cross section C_{sca} to absorption cross section C_{abs} as a function of total particle diameter, calculated via Mie theory. Line color, as indicated by legend, corresponds to percent of total diameter taken up by silica inner core. Index of refraction values used are $n_{\text{silica}} = 0.194 + 5.527i$, $n_{\text{silica}} = 1.44$, and $n_{\text{water}} = 1.33$ for the surrounding region. From [2]

procedure consists of using a polyethylene glycol (PEG) polymer chain functionalized at one end with orthopyridyl disulfide (OPSS) and at the other with an N-Hydroxysuccinimide ester (NHS). The OPSS-PEG-NHS is incubated with the antibody for 24 hours, in which time the NHS ester reacts with a lysine in the antibody, leaving the NHS ester free in solution and the antibody attached to the OPSS-PEG. This OPAb, as we call it, is then incubated with the gold for 24 hours, so that the OPSS group splits at the disulfide bond and the PEG chain attaches to the gold via a thiol bond, which has a strength slightly less than that of a covalent bond and much larger than that of a van der Waals bond !(appendix or footnote or reference on thiol bonds?). This should ensure that the antibody is firmly attached to the gold. The second part of the procedure is to prevent any other molecules from binding with the gold. This is accomplished by binding another PEG chain to the gold, of which one end is functionalized with a thiol group (SH) that then forms a thiol bond with the gold. This should fill on any space left after the addition of the OPAb.

Unfortunately, these tests also failed to produce the desired specific increase in scattering, so in Summer 2010 Oliver Hoidn and Perry Ellis '11 undertook a reexamination of the PEGylation protocol. Several significant results emerged from their studies that indicated problems with the PEGylation protocol. First, the gold nanoparticle solution, though its pH is advertised as between 6 and 8, was actually measured at a pH between 5 and 5.5 [3] due to the lack of a buffer in the solution. However, if commercial PBS is added, the salt in that solution screens the negative capping agent on the gold nanoparticles, thus preventing the mutual repulsion between the nanoparticles and causing them to agglomerate and fall out

of solution. To remedy this, a buffer solution made of $\text{Na}_2\text{HPO}_4 \cdot 7\text{H}_2\text{O}$ and $\text{NaH}_2\text{PO}_4 \cdot \text{H}_2\text{O}$ was added to the gold to achieve a total salt concentration of 10 mM. This concentration was chosen as it provides a sufficient level of buffering without screening the capping agent too much. However, over the course of the several days required for the PEGylation process, it was found that the gold still suffered from a high rate of agglomeration. A footnote was then found in Lowery et al. [7] that noted that PEG-SH cannot perform its protective function unless it has a molecular weight of at least 5 kDa. As the PEG-SH used up to that point had been of molecular weight 1.2 kDa, it had not protected the gold.

Thus, after Oliver and Perry concluded their work, it remained to readjust the PEGylation protocol for 5 kDa PEG-SH, and to use that updated protocol to once again try and get significantly specific contrast increase. To date, the PEGylation protocol has been optimized with the 5 kDa PEG-SH and produces results extremely consistent with the model of PEGylation we have developed. In addition, the 5 kDa PEG-SH appears to provide excellent long-term protection to the spheres. Spheres made with the optimized protocol have been used in two labeling experiments, which have provided further insights into the immunolabeling process.

2 Addition of Antibodies to Nanospheres

At the end of Summer 2010, Oliver Hoidn and Perry Ellis had determined that the optimal number of OPSS-PEG-antibody (OPAb) molecules per nanosphere was approximately 2000; however, there were significant concerns as to whether the OPSS-PEG-NHS (OPN) was successfully binding to the lysines on the antibody, or whether monolayer formation was simply the result of the antibodies binding to the nanospheres via van der Waals forces. The OPN reacts with a lysine by substituting the nitrogen atom in the NHS ester for the nitrogen atom on the functional group of the lysine (and their respective attached molecules, by proxy). A diagram of this reaction is shown in Figure 3.

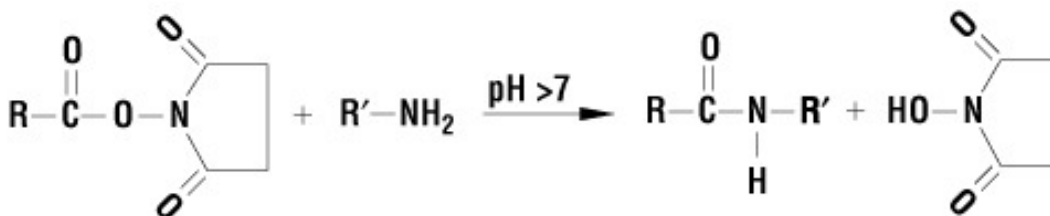


Figure 3: Schematic diagram of the OPN+antibody→OPAb reaction. **R** represents the OPSS-PEG, and **R'** represents the antibody. The reaction is favored in basic conditions. From [9]

Although the reaction requires a basic pH (>7) to run, basic conditions also favor a competing reaction, in which hydrolysis occurs and the NHS ester is replaced with a hydroxyl group. This renders the molecule unable to bind to antibodies, and the half-life of the hydrolysis reaction can be on the order of minutes at pH 8 [6]. Consequently, there was a concern that a large portion of the OPN used in the OPN+antibody→OPAb reaction was not binding to the antibody.

Fortunately, a direct physical measurement can be used to quantify the hydrolysis of the NHS ester. The free NHS ester in solution absorbs at 260 nm much more strongly than the

bound ester [8]. Therefore, the Cary 5000 UV-Vis Spectrophotometer was used to monitor the absorption at 260 nm over the course of several hours. The results of this measurement are shown in Figure 4.

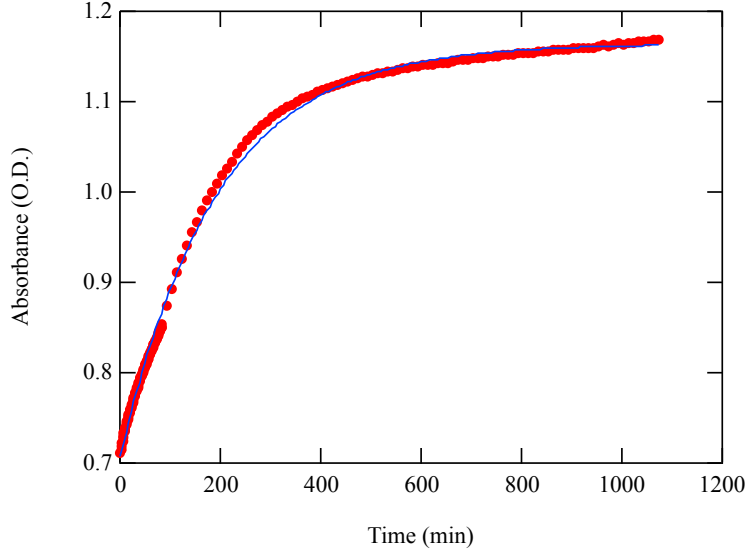


Figure 4: Plot of the absorbance of the OPN solution over time. The reaction rate seems to be proportional to concentration, giving a simple first-order rate law. The lower density of points at ~ 80 minutes occurred because the spectrophotometer was set to record a spectrum every 10 minutes rather than every 1 minute. The blue line displays a fit to $A = C_1 + C_2 e^{-C_3 t}$. The fitted values were $C_1 = 1.16$, $C_2 = -0.458$, and $C_3 = 0.00523$

Based on the coefficient of the exponent, $C_3 = 0.00523\text{s}^{-1}$, we can calculate that the half-life of NHS ester hydrolysis at pH 7.5 is

$$\tau_{1/2} = \frac{\ln 2}{C_3} = 133 \text{ min}$$

or about two hours.

Two conclusions can be drawn from this: first, there is very little danger of having no bound NHS remaining when the protein is added, since that should occur at the most 10 minutes after the OPN solution is created (and will most likely be less than five minutes after solution creation). Second, this confirms the need to incubate the protein with the OPN overnight. Since both hydrolysis of the NHS and the reaction with the lysine work on a similar mechanism, their rates can be expected to be comparable. Thus, in order to create as much OPAb as possible, at least four hydrolysis half-lives are necessary to achieve $> 90\%$ yield. However, since the hydrolysis is nontrivial on that time scale, we will use OPN should be used in a factor of 2 excess in order to facilitate maximal protein binding. Therefore, in the PEGylation procedure, we will use 2,000 antibodies per Au nanosphere

and 4,000 OPN molecules per nanosphere (see ??).

3 Addition of PEG-SH to Nanospheres

In the spring of 2011, several experiments were performed to characterize the 5 kDa PEG-SH (PS), which is used to provide protection to the Au nanospheres. The PS was characterized in three ways: a titration, a time study, and a protection study. These demonstrated that a number concentration of 50, 000 PS molecules per Au nanosphere, after 24 hours of incubation, should provide complete long-term protection to the Au nanospheres in a salt-rich environment.

3.1 Titration Study

A titration curve was made by adding 5 kDa PS to 90 nm gold nanospheres ($R=53$ nm) in varying concentrations, from 1000 PS per nanosphere to 10^7 PS per nanosphere. The hydrodynamic radii of these PEGylated nanospheres were then measured using the Dynamic Light Scattering (DLS) instrument, taking 15 30-second acquisitions of each solution and discarding the first three to account for temperature acclimation. This procedure was performed three separate times; a plot of the results is shown in Figure 5.

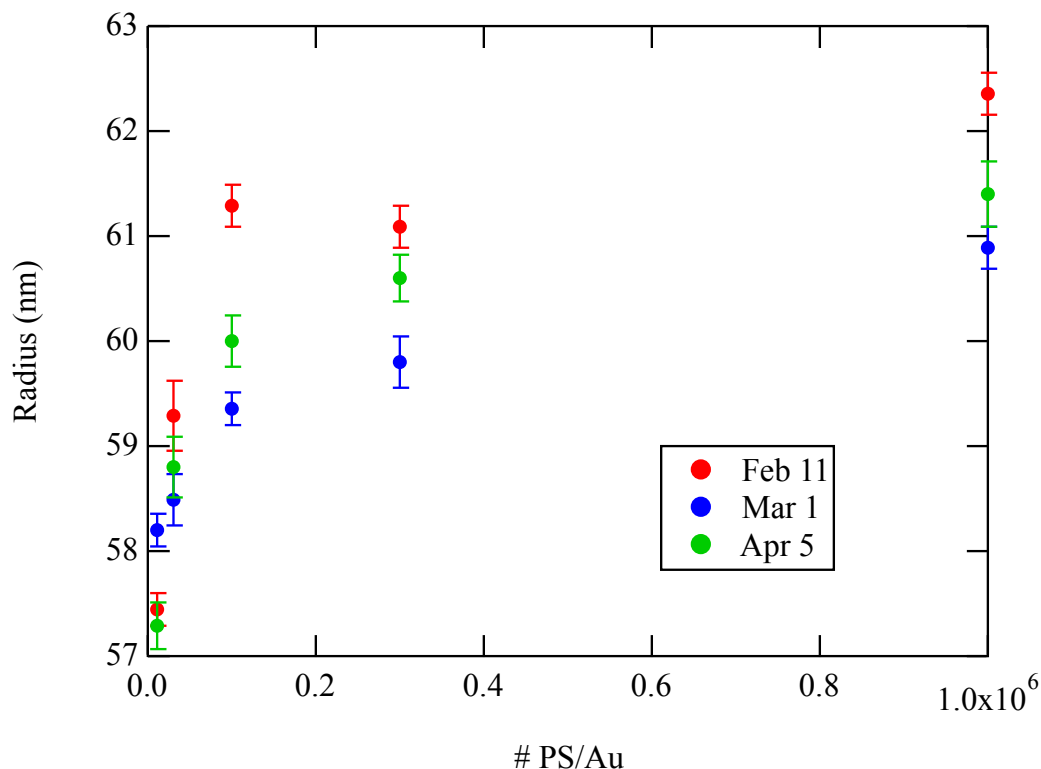


Figure 5: Plot of hydrodynamic radius of Au nanospheres with at various concentrations less than 30 minutes after addition of PS.

This plot shows the behavior of a rapid rise followed by a plateau that is expected of a species forming a monolayer on a surface. The plateau begins at approximately 50,000 PS molecules per nanosphere with R=60–61 nm, and has an elbow at around 10,000 PS per nanosphere.

A single 5 kDa PEG-SH molecule, with a density of $1.11 \frac{\text{g}}{\text{cm}^3}$, has a volume of

$$V_{5 \text{ kDa PEG-SH}} = \frac{5 \text{ kDa}}{1.11 \frac{\text{g}}{\text{cm}^3}} = 7.5 \text{ nm}^3$$

This means that a 5 kDa PEG-SH monolayer has, based on the change in hydrodynamic radius,

$$\#_{5 \text{ kDa PEG-SH}} = \frac{\frac{4}{3}\pi((60.5 \text{ nm})^3 - (51.5 \text{ nm})^3)}{V_{5 \text{ kDa PEG-SH}}} = 47,500 \text{ 5 kDa PEG-SH}$$

This indicates that the measurement of the plateau as beginning at 50,000 PEG-SH per nanosphere is correct. This also allows us to get a sense of the effective width (Prof. Haskell: word choice?) of a PEG-SH molecule as it sits on the gold. At monolayer concentration, the area on the surface of the gold taken up by each PEG-SH molecules is

$$A_{\text{PS}} = \frac{4\pi(51.5 \text{ nm})^2/\text{Au}}{47,500 \frac{\text{PS}}{\text{Au}}} = .70 \text{ nm}^2 = 70^2$$

This size is determined partially by the atomic size of the sulfur atom ($D = 2$), but mostly by the extent to which the PEG chain is bunched; clearly, most of the effective width comes from the bunching.

3.2 Time Study

The same samples used in the titration study were measured again after 48–72 hours of incubation, producing the radii shown in Figure 6.

The plateau in this graph is much sharper than in Figure 5, indicating that van der Waals forces and thiol bonding processes are in competition, with van der Waals binding dominating immediately after addition, but the lower-energy thiol bonds dominating after incubation time. This leads to the increased radius of the lower-radius samples and the decreased radius of the higher-radius samples. However, the plateau region still has R=60–61 nm, as a second indication of a monolayer. Clearly, it is essential that PEG-SH be allowed to incubate with spheres to allow for the PEG-SH binding to reach equilibrium.

3.3 Protection Study

As mentioned above, the main reason for using 5 kDa PEG-SH is to prevent the Au nanospheres from conglomeration. The Au nanosphere solution includes a negatively charged capping agent that makes the spheres repel each other; when the solution is buffered at pH ~ 7.5 to prevent antibodies from denaturing during the full immunogold procedure, positive ions are introduced into the solution that neutralize the capping agents, causing the gold nanospheres to agglomerate. Theoretically, PEG-SH would prevent this from happening, but 1 kDa PEG-SH does not, as shown in Figure 7.

Therefore, the protection capabilities of 5 kDa PS were tested by adding PEG-SH to the Au nanospheres in various concentrations, then mixing those solutions in equal volumes with

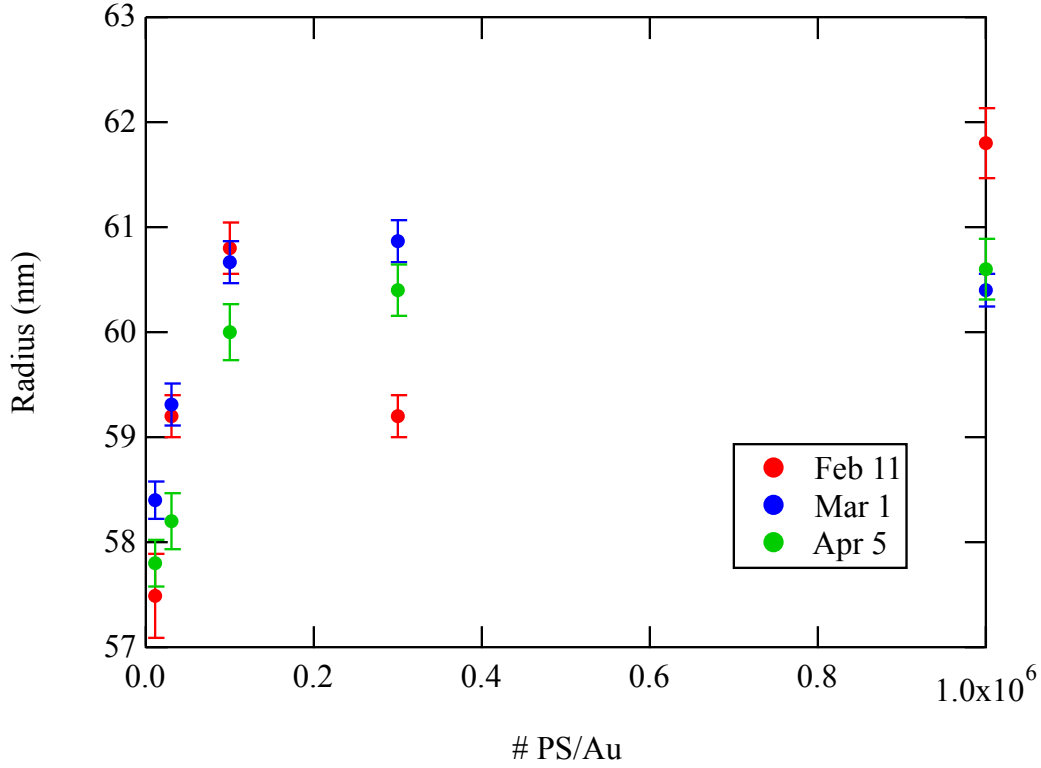


Figure 6: Plot of hydrodynamic radius of Au nanospheres with at various concentrations 48–72 hours after addition of PS.

commercial phosphate buffered saline. The spheres were allowed to incubate for at least 30 minutes with the PBS, then measured in the DLS. Selected results from those measurements are shown in Figure 8.

For all but the naked gold, almost all acquisitions are within 3 nm of the mean; this is also true of the 300k PS/Au without PBS from Summer 2010. However, with just 10k 5 kDa PS/Au, the width of the distribution barely widens when PBS is added—a stark contrast to the addition of PBS to 300k 1 kDa PS/Au. Furthermore, there was a ~ 15 nm increase in average radius between the 1 kDa PS spheres with and without PBS. In the case of the 10k 5 kDa PS/Au, the difference in average radius was negligible: 0.09 nm.

From observing the lack of change in both average radius and the change in radial distribution when using the 5 kDa PEG-SH, it is clear that the 5 kDa PEG-SH fully protects the Au nanospheres against capping agent neutralization. There is, however, a noticeable difference between the 10k and 300k PS/Au samples; the 300k is slightly narrower, indicating that it offers slightly more protection, consistent with the 300k PS/Au solution being

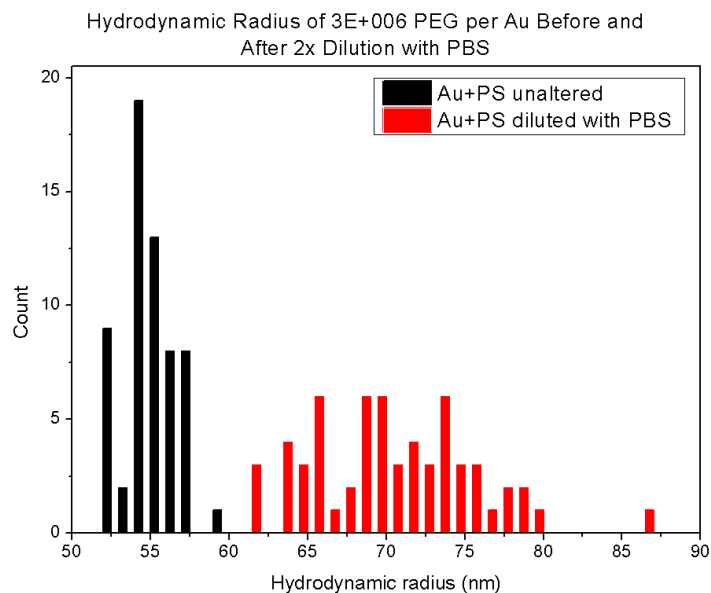


Figure 7: Histogram of radii of acquisitions of 300k 1 kDa PS/Au with and without PBS from Summer 2010. The distribution is noticeably shifted to the right and flattened after the addition of PBS. Data taken by Ellis and Hoidn [3].

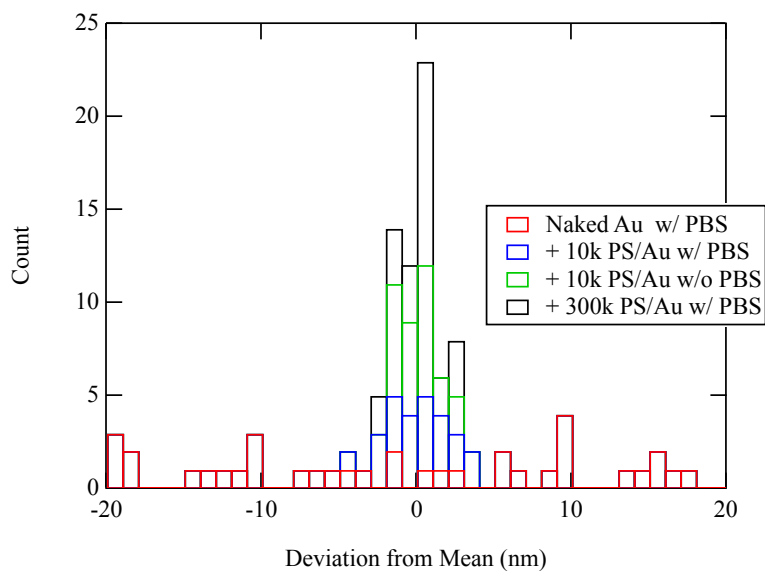


Figure 8: Stacked histograms of differing concentrations of Au-PS with and without PBS. The naked gold is significantly broader than any of the other distributions.

on the plateau while the 10k PS/Au is still on the rising part of the titration curve.

4 Results of the Full Protocol

Several fully labeled and protected nanosphere samples were created during the '11-'12 year. The protocol used was adapted from Oliver Hoidn and Perry Ellis's report [3], using 2,000 antibodies per Au nanosphere and the curve-elbow value 10,000 PEG-SH molecules per Au nanosphere. Detailed documentation of the protocol can be found in ??.

The progress of the protocol was monitored by a DLS radius measurement at five or six stages:

1. Immediately after the addition of the OPA_b
2. 24 hours after the addition of the OPA_b
3. Immediately after the addition of the PEG-SH
4. 24 hours after the addition of the PEG-SH
5. After dilution with equal parts PBS, to check for protection
6. (For most but not all samples) 48 hours after the addition of PEG-SH

The results of these measurements are shown in Figure 9. The data shows an immediate increase of 6–8 nm upon the addition of the OPA_b, followed by slight (<0.1 nm) gains after 24 hours of incubation. AP124F is an IgG antibody and has dimensions of approximately 14.5 nm × 8.5 nm × 4.0 nm [12] as shown in Figure 10; since the NHS replacement can occur on any lysine or N terminus (of which there are several), a 6–8 nm increase in radius is reasonable when all spatial orientations are taken into account.

An OPA_b conjugate should have a volume of

$$V = V_{\text{PEG}} + V_{\text{Ab}} = \frac{2.1\text{kDa}}{1.11 \frac{\text{g}}{\text{cm}^3}} + \frac{160\text{kDa}}{1.35 \frac{\text{g}}{\text{cm}^3}} = 200 \text{ nm}^3$$

Examining the hydrodynamic volume change after the addition of PEG-SH, this corresponds to

$$\frac{4}{3}\pi[(58 \text{ nm})^3 - (51.5 \text{ nm})^3]/200 \frac{\text{nm}^3}{\text{OPAb}} = 1230 \text{ OPAbs}$$

However, this is likely an under-estimate, as the 1.35 $\frac{\text{g}}{\text{cm}^3}$ density is for the crystalline state of protein [4]; the actual effective volume of the OPA_b in solution is likely larger. Further uncertainty is introduced by the complexity of the diffusion of an Au nanosphere with over 1000 OPA_b molecules attached to it. Therefore, this calculation serves primarily as an order-of-magnitude check; in that sense, 1230 OPA_b/Au compares quite favorably to the 2000 OPA_b/Au in solution.

We can again perform a calculation of effective width:

$$A_{\text{OPN}} = \frac{4\pi(51.5 \text{ nm})^2/\text{Au}}{1230 \frac{\text{OPAb}}{\text{Au}}} = 27.1 \text{ nm}^2$$

This is considerably larger than the effective width of the PEG-SH, indicating that the OPA_b molecules on the nanosphere sterically (word choice?) hinder other OPA_b molecules from forming thiol bonds with the nanosphere surface.

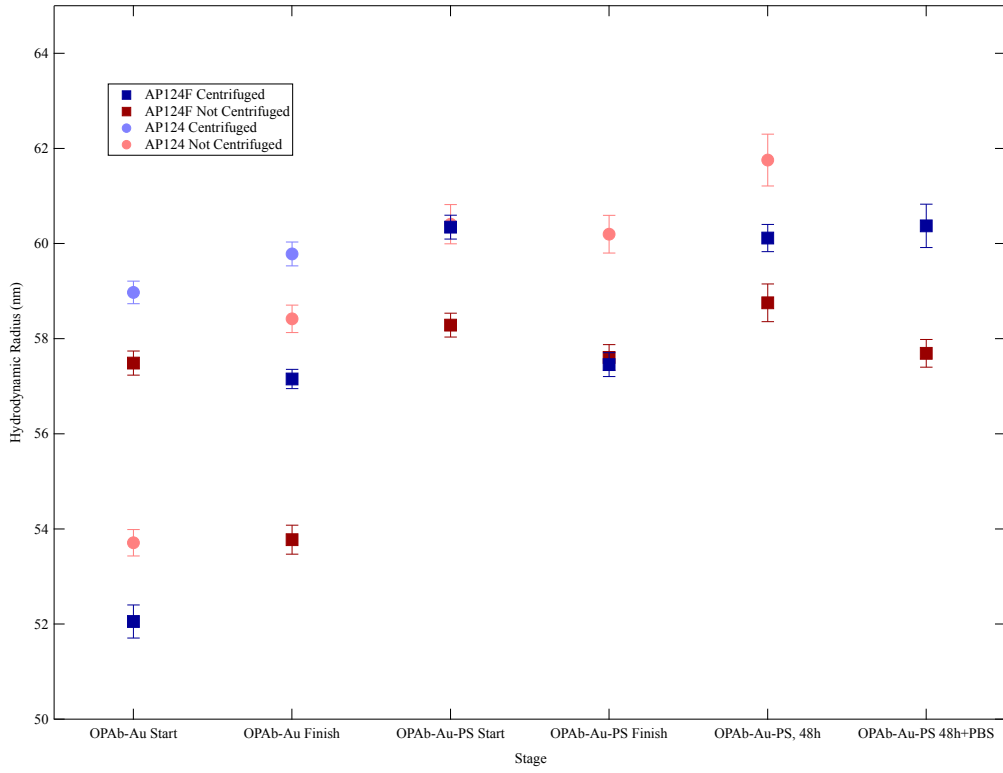


Figure 9: Plot of hydrodynamic radii of multiple solutions at each step in the protocol.
NOTE: PLACEHOLDER UNTIL I COLLABORATE ALL THE DATA.

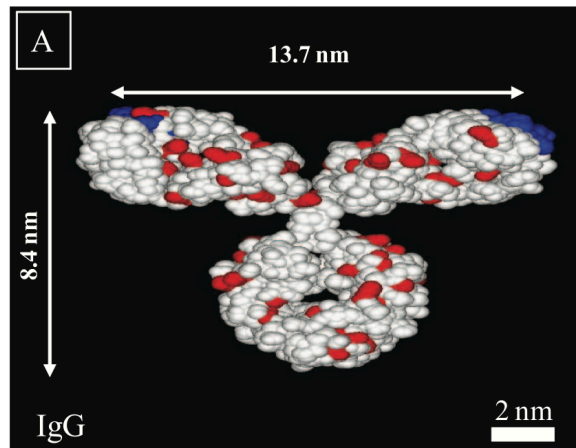


Figure 10: Structure dimensions of an IgG antibody. From [12].

Bibliography

- [1] Clarence W. C. Chan and Jamie L. Shoffeit. *Antibody-Gold Nanoparticle Conjugation for Immunogold Labeling in Optical Coherence Microscopy*. PhD thesis, Harvey Mudd College, May 2006. 3
- [2] David Coats. *Visualization of Cells and Cell Phenotype in Tissue-Engineered Corneas via Immunogold Labeling*. PhD thesis, Harvey Mudd College, 2008. 5
- [3] Perry Ellis and Oliver Hoidn. Pegylation of antibodies to gold nanospheres. August 2010. 5, 11, 12
- [4] Hannes Fischer, Igor Polikarpov, and Aldo F. Craievich. Average protein density is a molecular-weight-dependent function. *Protein Science*, 13(10):2825–2828, 2004. 12
- [5] National Eye Institute. Facts about the cornea and corneal disease. 3
- [6] Inc. Laysan Bio. Hydrolysis half-lives. 6
- [7] Amanda R Lowery, André M Gobin, Emily S Day, Naomi J Halas, and Jennifer L West. ImmunonanosHELLS for targeted photothermal ablation of tumor cells. *International Journal of Nanomedicine*, 1(2):149–154, 2006. 4, 6
- [8] T Miron and M Wilchek. A spectrophotometric assay for soluble and immobilized n-hydroxysuccinimide esters. *Analytical Biochemistry*, 126(2):433–435, 1982. 7
- [9] Pierce Protein Research Products. Chemistry of crosslinking. 6
- [10] Chris B. Raub, Elizabeth J. Orwin, and Richard C. Haskell. Immunogold labeling to enhance contrast in optical coherence microscopy of tissue engineered corneal constructs. In *Proceedings of the 26th Annual International Conference of the IEEE, Engineering In Medicine and Biology Society*, volume 1, pages 1210–1213, 2004.
- [11] Konstantin Sokolov, Michele Follen, Jesse Aaron, Ina Pavlova, Anais Malpica, Reuben Lotan, and Rebecca Richards-Kortum. Real-time vital optical imaging of precancer using anti-epidermal growth factor receptor antibodies conjugated to gold nanoparticles. *Cancer Research*, 63(9):1999–2004, 2003.
- [12] Yih Horng Tan, Maozi Liu, Birte Nolting, Joan G. Go, Jacquelyn Gervay-Hague, and Gang-yu Liu. A nanoengineering approach for investigation and regulation of protein immobilization. *ACS Nano*, 2(11):2374–2384, 2008. 12, 13
- [13] Robert Warren. *Immunogold Labeling of a Tissue-Engineered Cornea: Increasing the Binding Specificity of Immunogold Labeling via PEGylation*. PhD thesis, Harvey Mudd College, 2010. 4